

A Postmitotic Role for Isl-Class LIM Homeodomain Proteins in the Assignment of Visceral Spinal Motor Neuron Identity

Joshua P. Thaler,¹ Sonya J. Koo,¹
Artur Kania,² Karen Lettieri,¹
Shane Andrews,¹ Christopher Cox,²
Thomas M. Jessell,² and Samuel L. Pfaff^{1,*}

¹Gene Expression Laboratory
The Salk Institute

La Jolla, California 92037

²Howard Hughes Medical Institute

Department of Biochemistry
and Molecular Biophysics

Columbia University

New York, New York 10032

Summary

LIM homeobox genes have a prominent role in the regulation of neuronal subtype identity and distinguish motor neuron subclasses in the embryonic spinal cord. We have investigated the role of Isl-class LIM homeodomain proteins in motor neuron diversification using mouse genetic methods. All spinal motor neuron subtypes initially express both Isl1 and Isl2, but Isl2 is rapidly downregulated by visceral motor neurons. Mouse embryos lacking Isl2 function exhibit defects in the migration and axonal projections of thoracic level motor neurons that appear to reflect a cell-autonomous switch from visceral to somatic motor neuron character. Additional genetic mutations that reduce or eliminate both Isl1 and Isl2 activity result in more pronounced defects in visceral motor neuron generation and erode somatic motor neuron character. Thus, an early phase of high Isl expression and activity in newly generated motor neurons permits the diversification of visceral and somatic motor neuron subtypes in the developing spinal cord.

Introduction

The generation of neuronal diversity within the vertebrate central nervous system (CNS) depends on the specification of discrete sets of progenitor cells with restricted postmitotic neuronal fates (Briscoe et al., 2000; Desai and McConnell, 2000). Many aspects of neuronal phenotypic diversity are acquired only after cell cycle exit within sets of neurons that derive from an apparently uniform pool of progenitor cells (Jessell, 2000; Koo and Pfaff, 2002). These postmitotic steps of neuronal specification appear to control many of the differential properties of neurons that permit the establishment of appropriate migratory programs and axonal projections. At a molecular level, specific profiles of transcription factor expression have been shown to direct neuronal diversification (Brunet and Ghysen, 1999; Livesey and Cepko, 2001). One way to enhance the extent of neuronal diversity imposed by transcription factors involves the duplication of genes to encode

structurally related pairs of transcription factors with overlapping expression domains (True and Carroll, 2002). Many such transcription factor pairs have been shown to contribute to progenitor cell diversification (Briscoe and Ericson, 2001). But whether the coordinated expression of closely related transcription factor pairs also participates in the postmitotic diversification of neuronal subtypes is less well established.

The spinal cord and hindbrain represent regions of the vertebrate CNS in which some of the steps in neuronal diversification have been resolved, notably in the context of motor neuron generation and subtype diversification (Jessell, 2000; Pfaff and Kintner, 1998). In both the hindbrain and spinal cord, somatic and visceral motor neurons require Shh signaling for their differentiation (Ericson et al., 1997). In the hindbrain, somatic and visceral motor neurons emerge from different ventral progenitor domains, and thus the distinction in their phenotypic differentiation occurs early in the program of motor neuron generation (Ericson et al., 1997). In the spinal cord, however, somatic and visceral motor neurons are generated from a common set of ventral progenitor cells (Briscoe et al., 1999, 2000; Ericson et al., 1997). Yet, soon after their generation, postmitotic spinal motor neurons diversify into distinct functional subclasses (Jessell, 2000; Pfaff and Kintner, 1998; Shirasaki and Pfaff, 2002), although the mechanisms that control this process remain poorly defined.

The specification of somatic and visceral spinal motor neuron subtypes represents one of the most fundamental aspects of spinal motor neuron diversification. These two classes of motor neurons settle in different regions of the spinal cord, innervate different peripheral targets, and receive distinct presynaptic inputs (Levi-Montalcini, 1950; Lichtman et al., 1980; Markham and Vaughn, 1991). Somatic motor neurons are generated along the entire rostrocaudal axis of the spinal cord, settle in the ventral horn, and innervate skeletal muscle targets that mediate the voluntary control of movement. In contrast, visceral motor neurons of the sympathetic preganglionic motor column (PGC neurons) arise preferentially at thoracic levels, settle in the intermediate spinal cord, and participate in the autonomic control of a diverse array of visceral targets (Markham and Vaughn, 1991). The divergence of somatic and PGC neuronal identities becomes apparent prior to their migration to distinct settling positions within the spinal cord (William et al., 2003). During this period, molecular distinctions in motor neuron identity, most notably in the profile of expression of transcription factors, begin to emerge (Jessell, 2000; Shirasaki and Pfaff, 2002; Tsuchida et al., 1994).

In vertebrates, six pairs of structurally related LIM homeodomain proteins have been defined, with each protein pair typically exhibiting an overlapping profile of expression (Hobert and Westphal, 2000). Strikingly, four LIM homeodomain protein pairs have been shown to function at several sequential steps during motor neuron differentiation: in neuronal fate specification, neuronal migration, and axonal pathfinding (Shirasaki and Pfaff, 2002). The LIM homeodomain protein pair Lhx3 and

*Correspondence: pfaff@salk.edu

Lhx4 acts in a redundant manner in determining the differentiation of two major sets of motor neurons that project their axons out of the CNS via dorsal or ventral exit points (Sharma et al., 1998). This basic anatomical feature distinguishes most somatic motor neurons from visceral motor neurons in the hindbrain (Lumsden and Krumlauf, 1996). But in the spinal cord, both somatic and visceral motor neurons project their axons through a ventral exit point, and consistent with this, the distinction between somatic and visceral neuronal fate is independent of the actions of Lhx3 and Lhx4 (Sharma et al., 1998). Instead, another LIM homeodomain pair, the Isl1 and Isl2 proteins, distinguishes somatic and visceral motor neurons (Tsuchida et al., 1994; Varela-Echavarría et al., 1996), raising the possibility that the Isl proteins are involved in this aspect of motor neuron diversification. By the time individual subclasses of motor neurons have settled in different locations within the chick spinal cord, most somatic motor neurons coexpress Isl2 and Isl1, whereas PGC neurons express Isl1 but not Isl2 (Tsuchida et al., 1994). The functional significance of this distinction in Isl expression profile in somatic and PGC neurons, however, remains unclear. Analysis of *Isl1* null mutant mice has not been informative in this context, since motor neurons die before their diversification becomes evident (Pfaff et al., 1996).

We have used genetic studies in the mouse to examine the contribution of the Isl-class LIM homeodomain protein pair to the postmitotic diversification of visceral and somatic motor neurons in the developing spinal cord. We find that both Isl proteins are initially expressed by all postmitotic spinal motor neurons prior to the diversification of somatic and visceral neuronal fates and that somatic but not visceral motor neurons maintain Isl2 expression at later embryonic stages. Nevertheless, our genetic data show that this early phase of Isl2 expression by prospective PGC neurons is critical for the emergence of complete visceral motor neuron character. In *Isl2* mutant embryos, thoracic level motor neurons settle in aberrant locations and exhibit defects in their peripheral axonal trajectory. These defects appear to have their basis in a cell-autonomous impairment in PGC neuronal specification with the consequence that additional motor neurons possess a somatic-like character. In addition, in *Isl2;Hb9* compound mutant mice, a genetic context in which the expression of Isl1 and Isl2 is lost in postmitotic motor neurons, there is a virtually complete absence of PGC neurons, yet motor neuron neurotransmitter status and axonal projections into the periphery are maintained. Our findings show that a brief period of Isl2 activity in newly generated motor neurons is a key requirement for the diversification of motor neuron subtypes, in particular permitting the progression of neurons to a PGC neuronal character.

Results

Isl2 Expression in Mouse Embryonic Spinal Cord

To help monitor the fate, position, and axonal projections of motor neurons in the developing spinal cord, we generated a mouse line in which a tauLacZ (TLZ) fusion cassette (Callahan et al., 1998) was targeted to

the 3'-untranslated region of *Isl2* (*Isl2*^{TLZ}) (Figure 1A). To achieve coincident expression of Isl2 and the fusion cassette, a bicistronic mRNA was created using an internal ribosome entry sequence (IRES) to facilitate tauLacZ translation (Mombaerts et al., 1996). Analysis of *Isl2*^{TLZ} embryos at E13.5 revealed LacZ expression in spinal motor neurons and dorsal root ganglion neurons (Figure 1B). At hindbrain levels, motor neurons in the abducens (VI) and hypoglossal (XII) nuclei expressed LacZ, as did sensory neurons in the trigeminal (V) and vagal (X) sensory ganglia (Figure 1C, data not shown). This pattern of LacZ expression resembles the profile of Isl2 expression in chick (Varela-Echavarría et al., 1996).

We used the *Isl2*^{TLZ} line in combination with immunohistochemistry to explore the developmental relationship between Isl1, Isl2, and Hb9 expression in developing spinal motor neurons. All newly generated motor neurons coexpressed Hb9 and Isl1 as they emerge from the ventricular zone (Arber et al., 1999; Ericson et al., 1992; Thaler et al., 1999). In contrast, at E9.5, Isl2 expression was not detected in motor neurons until they migrated laterally (Figures 1D and 1E). Thus, Isl2 expression begins after that of Hb9 and Isl1. However, by E10.5, Isl2 is expressed in all spinal motor neurons (Figure 1F).

We next examined the extent of overlap in expression of Isl2, Isl1, and Hb9 at E13.5, when the distinction between somatic and visceral motor neuron subtypes is readily apparent. At this stage, the level of each Isl protein varied among motor neuron subtypes (Figures 1G–1I). In particular, PGC neurons appeared to express markedly lower levels of Isl2 than Isl1. Since tauLacZ is a stable protein, its perdurance can be used to infer prior phases of gene expression (Echelard et al., 1994). We therefore examined *Isl2*^{TLZ} mice to assess whether the weak Isl2 labeling in PGC neurons reflects an early transient phase of Isl2 expression. At E13.5, LacZ was detected in the axons of PGC neurons, defined by expression of the neuronal form of nitric oxide synthase (nNOS) expression (Figures 1J and 1K) (Wetts and Vaughn, 1994). These findings suggest that PGC motor neurons coexpress Isl2 and Isl1 shortly after their generation at E9.5 but downregulate Isl2 expression as they mature and settle in the intermediate region of the spinal cord (Figure 1L). The level of Isl2 expression also varied considerably within the MMC, where high levels of Isl2 were detected in the medial (m) division with much lower levels in the lateral (l) division (Figure 1I).

A Disruption in the Motor Neuron Settling Pattern in *Isl2* Mutant Mice

To begin to examine the role of Isl2 in the differentiation of spinal motor neurons, we generated a null mutation in the *Isl2* gene, replacing the three exons encoding the homeodomain and C terminus with a *neomycin* cassette (Figure 2A). Homozygous *Isl2* embryos lacked Isl2 protein expression (Figures 2B and 2C) and thus appear to be null mutants. *Isl2* homozygous mutant mice were born with no overt morphological defects but displayed severe abdominal distension, and nearly all died within 24 hr of birth (see Supplemental Figures S1A and S1B at <http://www.neuron.org/cgi/content/full/41/3/337/DC1>).

The early steps in the differentiation of spinal motor neurons appeared normal in *Isl2* mutants as assessed by

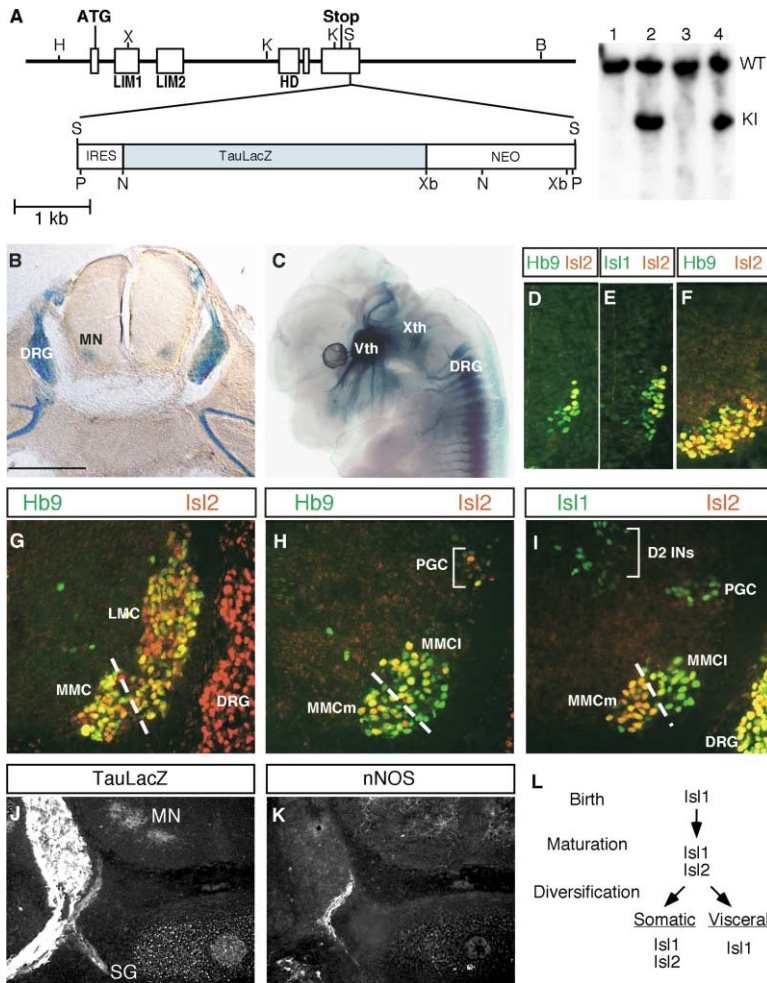


Figure 1. Isl2 Expression in Motor Neuron Subtypes

(A) Gene targeting strategy used to generate *Isl2^{TLZ}* mice. The ES DNA for the Southern blot was digested with HindIII and NcoI to reveal the wild-type (WT) 10 kb allele and a knockin (KI) allele of 6 kb in lanes 2 and 4. H, HindIII; X, XhoI; K, KpnI; S, SphI; B, BglII; P, PacI; N, NcoI.

(B) X-gal staining labels dorsal root ganglia (DRG) and motor (MN) axons in E13.5 *Isl2^{TLZ}* embryos.

(C) Side view of cleared *Isl2^{TLZ}* embryo reveals heavy expression in the trigeminal (Vth) and vagal (Xth) sensory ganglia. DRGs at each spinal cord segment are visible from this view.

(D and E) Expression of Hb9, Isl1, and Isl2 monitored in E9.5 mouse thoracic spinal cord. Both Hb9 and Isl1 are expressed in medial cells lacking Isl2, indicating they precede Isl2 expression in motor neurons.

(F) By E10.5, Isl2 is coexpressed with Hb9 in all motor neurons.

(G–I) Double-label immunocytochemistry on E13.5 mouse right ventrolateral quadrant spinal cords.

(G) Hb9 and Isl2 are coexpressed in brachial level motor neurons including MMC and LMC cells. DRG neurons express only Isl2.

(H) At thoracic levels, Hb9 and Isl2 appear in the two halves of the MMC (MMCm and MMCi) and at low levels in some PGC cells (bracket).

(I) Isl1 and Isl2 are expressed in the MMCm and MMCi in inverse proportion. D2 INs express only Isl1, while the DRG expresses high levels of both proteins.

(J) LacZ antibody labeling of E13.5 *Isl2^{TLZ}* embryos reveals reporter expression in the DRG, motor neurons within the spinal cord, and visceral motor axons projecting toward the sympathetic ganglia (SG).

(K) A serial section to that shown in (J) labeled with nNOS antibody specifically marks visceral motor axons.

(L) Schematic outlining the temporal expression of the *Isl* genes during postmitotic stages of motor neuron development. Scale bar, 400 μ m (B), 700 μ m (C), 100 μ m (D and E), 95 μ m (F), 105 μ m (G–K).

expression of the cholinergic neurotransmitter marker protein, vesicular acetylcholine transporter (VAcHT), and by the retrograde labeling of motor neurons after rhodamine-dextran injection into peripheral muscle targets (see Supplemental Figures S1E–S1H at <http://www.neuron.org/cgi/content/full/41/3/337/DC1>). At cervical and lumbar levels of the spinal cord, motor neurons exhibited normal migratory and settling patterns (Supplemental Figures S1I and S1J) and projected axons along appropriate pathways (Supplemental Figures S1E–S1H, data not shown). Similarly, at hindbrain levels, somatic cranial motor nuclei of the Vth and XIIth that normally express Isl2 appeared to develop normally in its absence (Supplemental Figures S1C and S1D) (Varela-Echavarría et al., 1996).

Several defects in motor neuron differentiation were, however, observed at thoracic levels of the spinal cord. Many Hb9⁺ motor neurons were found in ectopic locations, either in intermediate areas of the spinal cord or within the ventral roots (Figures 2D–2G). In addition, the tight columnar organization of median motor column (MMC) neurons evident at thoracic levels of wild-type

embryos was disrupted in *Isl2* mutants, with an intermingling of neurons in the medial and lateral divisions of the MMC, defined by their Lhx3/Hb9 expression status (Figures 2H and 2I).

Impairment of Visceral Motor Neuron Differentiation in *Isl2* Mutants

To address the basis of the motor neuron positioning defects observed in *Isl2* mutants, we analyzed the properties of the ectopic Hb9⁺ neurons found in the intermediate region of the thoracic spinal cord. By E13.5, ectopic Hb9⁺ neurons were intermingled with Chx10⁺ V2 interneurons (Figures 3A and 3B) but still extended axons into the periphery (Figures 3C and 3D). To begin to address whether the ectopic location of Hb9⁺ motor neurons results from a defect in motor neuron subtype differentiation, we examined the expression of markers that distinguish newly differentiated motor neurons (Sharma et al., 1998). Many ectopic Hb9⁺ motor neurons expressed Lhx3, a marker of medial MMC motor neurons (Figures 3E and 3F). Strikingly, however, most of these ectopically located neurons lacked Isl1 expres-

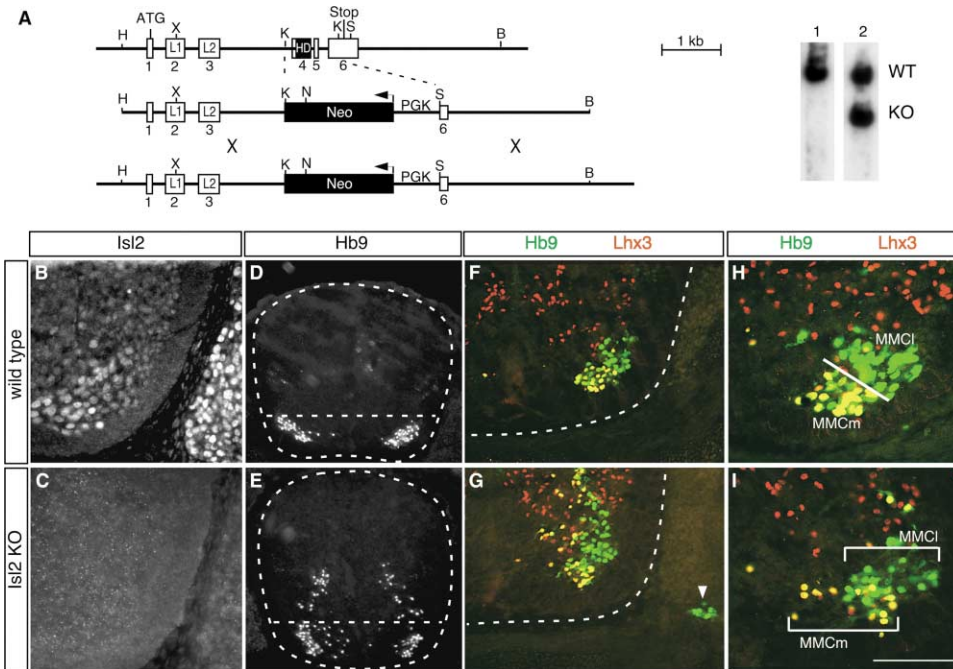


Figure 2. *Isl2* Mutant Embryos Exhibit Motor Neuron Migration Defects

(A) Diagram illustrating the generation of the *Isl2* knockout mouse. Top line indicates the genomic *Isl2* locus. The LIM domains and HD have been marked in exons 2–4. Middle line shows targeting construct with a PGK-NEO cassette transcribed in the reverse orientation to the *Isl2* gene. Bottom line shows recombined locus. The Southern blot was performed by digesting ES DNA with HindIII and NcoI to reveal the 10 kb wild-type (WT) and 7 kb knockout (KO) alleles. H, HindIII; X, XhoI; K, KpnI; N, NcoI; S, SphI; B, BglII. (B–I) Double-label immunohistochemical staining of right ventral quadrant E13.5 mouse embryo spinal cords. (B and C) *Isl2* antibody staining reveals *Isl2* expression in wild-type motor and DRG neurons, but fails to detect *Isl2* in knockout embryos, confirming the generation of a null mutant. (D and E) *Hb9* immunostaining reveals an inappropriate dorsomedial migration of cells in the thoracic spinal cord of *Isl2* knockout embryos. (F and G) In *Isl2*-deficient embryos, a subgroup of *Hb9*⁺ cells migrate from the neural tube and settle in the ventral root (arrowhead). (H) In wild-type embryos, cells within the MMCI (*Hb9*⁺, green) and MMCm (*Hb9*⁺/*Lhx3*⁺, yellow) segregate into distinct columnar positions. (I) In *Isl2* mutants, the MMCI and MMCm columns are less organized with intermingling of different motor neuron subtypes. Scale bar, 80 μ m (B, C, H, and I); 320 μ m (D and E); 160 μ m (F and G).

sion at E13.5 (Figures 3G and 3H). We therefore examined the status of *Isl1* expression during the initial stages of postmitotic motor neuron differentiation. At E9.5, *Isl1* expression was indistinguishable in mutant and wild-type embryos, but by E10.5 in *Isl2* mutants, *Isl1* expression was absent from a small group of medially positioned motor neurons (data not shown). By E11.5, the spatial segregation between *Hb9*⁺/*Isl1*⁺ and *Hb9*⁺/*Isl1*⁻ cells became more distinct as *Hb9*⁺/*Isl1*⁻ neurons began to migrate dorsally (Figures 3I and 3J). These results therefore reveal a temporal correlation between the downregulation of *Isl1* and the ectopic dorsal positioning of thoracic level motor neurons.

The detection of ectopic *Hb9*⁺ motor neurons exclusively at thoracic levels of *Isl2* mutant embryos raised the question of whether their appearance reflects a perturbation in the differentiation of PGC and/or lateral MMC neurons, the two motor neuron subtypes generated selectively at thoracic levels of the spinal cord (Sharma et al., 1998). To address this issue, we quantified motor neuron columnar subtypes at different rostrocaudal levels of the spinal cord using transcription factor markers (Table 1). The total number of motor neurons at brachial, lumbar, and thoracic levels was similar in wild-type and *Isl2* mutants (Table 1). Consistent with this, the number of TUNEL⁺ cells in the thoracic spinal

cord was unchanged in *Isl2* mutants examined from E10.5 to E13.5 (data not shown). Thus, the overall motor neuron number is not altered in *Isl2* mutants.

We therefore examined whether the assignment of motor neuron subtype identity was altered in *Isl2* mutants. The eventual restriction of *Isl2* to somatic motor neurons (Tsuchida et al., 1994; Varela-Echavarría et al., 1996) suggested the possibility of a somatic-to-visceral conversion in motor neuron fates in *Isl2* mutants (see Figure 1L). However, the ectopic *Hb9*⁺ neurons observed in *Isl2* mutants lacked the PGC marker nNOS (Figures 3K and 3L), arguing against this idea. Instead, and somewhat counterintuitively, we detected a 4.8-fold decrease in the number of *Isl1*⁺/nNOS⁺ PGC-like motor neurons in *Isl2* mutants, compared to wild-type embryos (mean 17/section versus 80/section) (Figures 4A–4D, Table 1). Conversely, there was a significant increase in the number of motor neurons expressing the somatic markers *Hb9* and *Lhx3* at thoracic levels of *Isl2* mutant mice (Figures 4E–4H, Table 1).

To examine the subtype identity of the extra somatic-like motor neurons detected at thoracic levels, we first tested whether PGC neurons had converted into lateral MMC motor neurons, since this somatic motor neuron class is generated selectively at thoracic levels of the spinal cord. The loss of PGC neurons in *Isl2* mutants

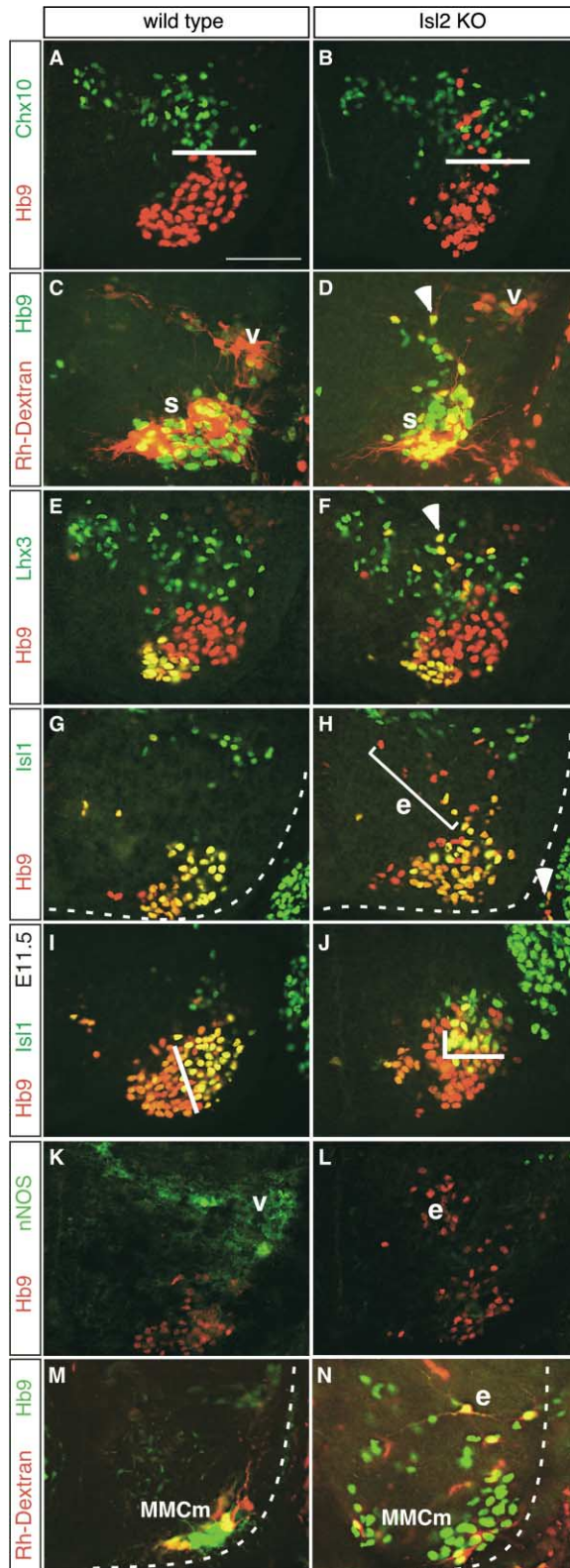


Figure 3. Ectopically Located Cells Exhibit MMCm-like Characteristics
(A–H) Double-label immunohistochemical staining of right ventral quadrant E13.5 mouse embryo spinal cords.
(A and B) Ectopically located Hb9⁺ cells do not express the V2 interneuron marker Chx10.
(C and D) Rhodamine-dextran-filled peripheral nerve labels the ec-

Table 1. Quantification of Motor Neuron Subtypes

| Brachial | Thoracic | Lumbar |
|--------------------|--------------------|--------------------|
| Somatic MN | Somatic MN | Somatic MN |
| +/- 2738 | +/- 3759 | +/- 1870 |
| -/- 3084 | -/- 5374 | -/- 1498 |
| (n = 11) | (n = 30) | (n = 6) |
| Visceral MN | Visceral MN | Visceral MN |
| +/- 20 | +/- 1758 | +/- 30 |
| -/- 0 | -/- 377 | -/- 10 |
| (n = 11) | (n = 22) | (n = 5) |

Thoracic Motor Neuron Subtypes

| Total Number | Number/sect. ± SD |
|----------------|-------------------|
| PGC | PGC |
| +/- 1758 | +/- 80 ± 17 |
| -/- 377 | -/- 17 ± 10 |
| (n=22) | |
| MMCm | MMCm |
| +/- 1226 | +/- 42 ± 14 |
| -/- 1307 | -/- 45 ± 13 |
| (n=29) | |
| MMCI | MMCI |
| +/- 1827 | +/- 63 ± 16 |
| -/- 2096 | -/- 72 ± 29 |
| (n=29) | |
| Ectopic | Ectopic |
| +/- 0 | +/- 0 |
| -/- 1066 | -/- 35 ± 18 |
| (n=30) | |
| All MNs | All MNs |
| +/- 4439 | +/- 202 ± 34 |
| -/- 4285 | -/- 195 ± 47 |
| (n=22) | |

Immunocytochemistry on 15 μm sections taken at 100 μm intervals was used to identify motor neuron subtypes in E13.5 heterozygous and *Isl2* mutant littermates. Hb9 was used to label somatic motor neurons, and Isl1/nNOS coexpression was used to identify visceral motor neurons (PGC cells). The somatic motor neurons were subdivided into MMCm and MMCI based on their Lhx3 status, and ectopic motor neurons were defined based on the identification of dorsally located Hb9⁺/Lhx3⁺ cells. Mean ± SD cell number calculated from one embryo of each genotype. Results representative of >6 embryos.

was, however, not offset by an increase in lateral MMC neuronal number, as assessed by LIM homeodomain protein expression profiles (Table 1). Thus, the depletion of visceral motor neurons in *Isl2* mutants appears to be compensated for primarily by the appearance of atypical and ectopically positioned somatic-like Hb9⁺/Lhx3⁺/

topic Hb9⁺ cells in *Isl2*-deficient embryos (arrowhead) in addition to the somatic (s) and visceral (v) motor neurons. (E and F) Ectopically located Hb9⁺ motor neurons express Lhx3 in *Isl2*-deficient embryos (arrowhead) like the MMCm motor column. (G and H) Most dorsomedial ectopic Hb9⁺ cells (e) fail to express Isl1 at E13.5, but those in the ventral root show mixed genetic profiles (arrowhead).

(I and J) By E11.5, the motor columns have coalesced with clear distinctions in expression patterns of Isl1 and Hb9. The downregulation of Isl1 is more pronounced by this stage (fewer yellow double-labeled cells in *Isl2* knockout embryos).

(K and L) At E13.5, ectopically located Hb9⁺ cells (e) do not express the visceral (v) motor neuron marker nNOS (Wetts and Vaughn, 1994).

(M and N) Rhodamine-dextran fills from axial muscles label MMCm and ectopic (e) Hb9⁺ cells in *Isl2* mutants. Scale bar, 80 μm (A–N).

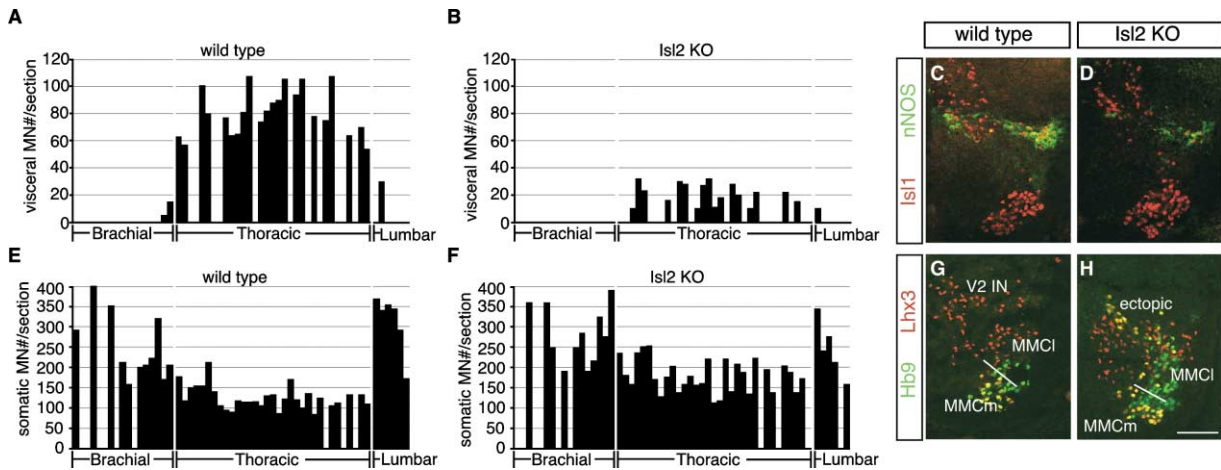


Figure 4. Increased Numbers of Somatic Motor Neurons in *Isl2* Knockouts

(A, B, E, and F) Quantitative analysis of somatic and visceral motor neuron types in E13.5 embryos. Somatic motor neurons were counted based on Hb9 reactivity, and visceral motor neurons were detected as *Isl1*⁺/*nNOS*⁺ cells. Sections were 15 μ m and were collected every 100 μ m. Missing bars represent an uncounted section, not a zero value.

(A) Visceral motor neurons in wild-type embryo.

(B) Visceral motor neurons in an *Isl2* knockout embryo.

(E) Somatic motor neurons in a wild-type embryo.

(F) Somatic motor neurons in an *Isl2* knockout embryo.

(C, D, G, and H) Double-label immunocytochemistry on thoracic level right ventral quadrant spinal cords from E13.5 embryos.

(C) Wild-type labeling of *Isl1*⁺/*nNOS*⁺ visceral motor neurons.

(D) Fewer *Isl1*⁺/*nNOS*⁺ visceral motor neurons are detected in *Isl2* knockout embryos.

(G) Wild-type MMCm and MMCI columns demarcated by the presence or absence of *Lhx3* in *Hb9*⁺ cells.

(H) *Isl2* knockout embryos have ectopically located *Hb9*⁺/*Lhx3*⁺ MMCm-like cells and a slightly enlarged *Hb9*⁺ MMCI population. Scale bar, 80 μ m (C, D, G, and H).

Isl1⁻ neurons (35 ± 18 per section in *Isl2* mutant embryos versus zero per section in wild-type embryos) (Table 1). Ectopically positioned *Hb9*⁺ neurons were retrogradely labeled after injection of rhodamine-dextran into axial muscles in *Isl2* mutants (Figures 3M and 3N), providing further evidence of the somatic properties of these neurons.

Although the ectopically positioned motor neurons in *Isl2* mutant mice exhibit somatic characteristics, some PGC neuronal traits were retained by these cells. First, ectopic thoracic motor neurons, as with PGC neurons, settled at a position dorsal to normal somatic motor neurons (Barber et al., 1998; Markham and Vaughn, 1991). Second, the small size of the nuclei of these ectopic motor neurons is characteristic of visceral rather than somatic motor neurons (Phelps et al., 1988; Wetts and Vaughn, 1994). In *Isl2* mutants, ventrally located somatic motor neurons had a mean nuclear diameter of 8.0 ± 0.6 μ m, whereas the nuclear diameter of ectopic motor neurons was 5.5 ± 0.5 μ m ($p < 0.01$), similar to that of PGC neuronal nuclei. The hybrid PGC-somatic character of ectopic *Hb9*⁺/*Lhx3*⁺/*Isl1*⁻ neurons provides indirect support for the idea that they are derived from motor neurons normally fated to become PGC neurons rather than from a somatic motor neuron population.

A Cell-Autonomous Influence of *Isl2* Underlies the Selection of Somatic and Visceral Motor Neuron Fates

Many of the genes that specify motor neuron subtype fates act in a cell-autonomous manner (Shirasaki and

Pfaff, 2002). However, nonautonomous interactions have also been implicated in the specification of motor neuron identity. For example, the differentiation of *Lim1*⁺ lateral LMC neurons depends on retinoids supplied by adjacent LMC neurons (Sockanathan and Jessell, 1998). Since *Isl2* is initially expressed by both somatic and visceral motor neurons, it remained unclear whether appropriate PGC neuronal differentiation requires *Isl2* intrinsically or whether the influence of *Isl2* might be indirect, perhaps reflecting a requirement in somatic motor neurons for the production of a nonautonomous signal that directs PGC neuronal differentiation.

To address the autonomy of *Isl2* function in PGC neuronal specification, we monitored motor neuron subtype differentiation in chimeric mouse embryos composed of wild-type and *Isl2* mutant cells in different proportions. In a first set of chimeras, we analyzed PGC neuronal differentiation under conditions in which a small minority of wild-type PGC neurons were present in a predominantly *Isl2* mutant cellular context. Wild-type motor neurons were derived from the mouse strain *Tg(Hb9-nLacZ)* (Sharma et al., 2000) and identified by virtue of nuclear (n) LacZ expression. Control embryos in which wild-type nLacZ⁺ motor neurons were interspersed with heterozygous *Isl2* mutant cells showed no evidence of inappropriate migration (data not shown). In chimeric embryos comprising 10%–20% wild-type (nLacZ⁺) cells and 80%–90% *Isl2* mutant cells, we also found no evidence for the inappropriate migration of wild-type (nLacZ⁺) motor neurons (0/184 nLacZ⁺ neurons detected in ectopic locations; Figures 5A–5D). Thus, a preponderance of *Isl2*-deficient motor neurons

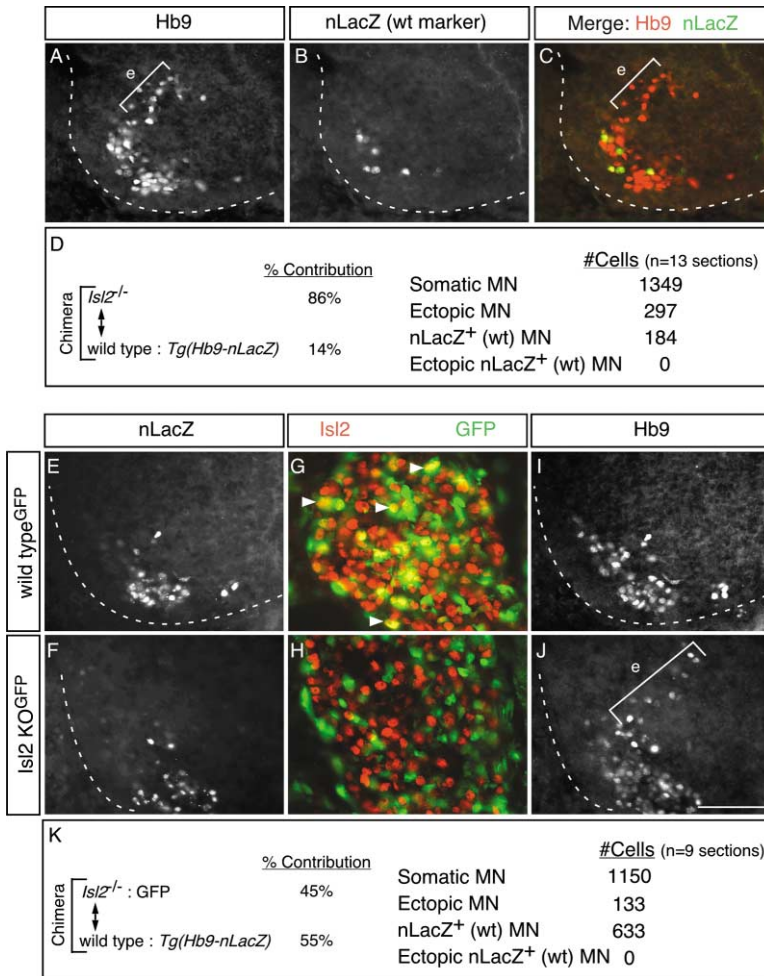


Figure 5. *Isl2* Functions Cell Autonomously (A–D) Aggregation chimeras were formed between *Isl2*^{-/-} embryos and wild-type embryos carrying the *Tg(Hb9-nLacZ)* transgene. In this group, we selected chimeras that were mainly comprised of *Isl2*^{-/-} cells, which was confirmed by a lack of *Isl2* immunoreactivity (data not shown). Motor neuron (MN) gene expression profiles and cell body positions were monitored in E13.5 embryos.

(A) Hb9 expression was used to quantify somatic and ectopic motor neuron number in (D). (B) nLacZ expression was used to monitor the number and position of wild-type motor neurons.

(C) The ratio of Hb9⁺ to nLacZ⁺ cells was used to determine the percent contribution of *Isl2*^{-/-} and wild-type cells in (D), respectively. (D) Quantitative analysis of motor neuron types and positions. Ectopically located motor neurons were defined as having cell bodies located dorsal-medial to the normal ventral-horn location for these cells (see [e] in [A] and [C]). No wild-type (nLacZ⁺) motor neurons were found to migrate into ectopic locations. Data representative of nine chimeras of this type.

(E–K) These aggregation chimeras contained cells from two sources: GFP-marked cells from embryos produced by intercrossing *Tg(βactin-GFP)*, *Isl2*^{+/-} mice, and LacZ-marked wild-type cells from embryos produced by intercrossing *Tg(Hb9-nLacZ)* mice. We selected E13.5 chimeric embryos in which a majority of motor neurons were derived from the nLacZ⁺ donor.

(E, G, and I) Marker expression in a chimeric embryo with wild-type GFP-marked cells and wild-type LacZ-marked motor neurons.

(F, H, J, and K) Marker expression in chimeric embryo with *Isl2*^{-/-}:GFP-marked cells and wild-type LacZ-marked motor neurons.

(E and F) nLacZ-marked motor neurons (wild-type) are located in normal positions in chimeric embryos containing GFP⁺/*Isl2*^{-/-} motor neurons.

(G and H) Double labeling with *Isl2* and GFP reveals the *Isl2* status of the GFP-marked donor embryos. Wild-type DRG cells coexpress *Isl2* and GFP (yellow, arrowheads) while GFP⁺ cells derived from an *Isl2*^{-/-} embryo do not express *Isl2*.

(I) Hb9 expression shows that somatic motor neurons are located in normal positions.

(J) Hb9 labeling detects ectopically located somatic motor neurons (e) in chimeras with *Isl2*-deficient cells.

(K) Quantification of marked motor neurons reveals that LacZ⁺ wild-type motor neurons do not rescue (prevent) the ectopic migration of *Isl2*^{-/-} somatic motor neurons. Data representative of four chimeras of this type. Scale bar, 80 μm (A–C, E, F, I, and J), 55 μm (G and H).

does not obviously influence the normal development and migratory pattern of wild-type motor neurons.

To test, conversely, whether signals provided by wild-type motor neurons can suppress the aberrant migratory behavior of *Isl2* mutant thoracic motor neurons, we examined a second group of chimeras in which wild-type cells outnumbered *Isl2* mutant cells. To assign the genotypes of neurons within these chimeras, we crossed *Isl2* mutant mice with a line bearing a ubiquitously expressed GFP transgene, *Tg(βactin-GFP)* (Ikawa et al., 1998). The GFP-marker line helped to quantify the level of chimerism and provided a marker for neurons that originated from *Isl2* mutant embryos. This step was necessary because the embryos in this group were comprised mainly of wild-type cells, making it difficult to distinguish chimeras made with *Isl2*^{+/+} and *Isl2*^{+/-} cells from those with *Isl2*^{-/-} cells. Individual neurons within these embryos were genotyped by double-label immunofluorescence

to determine whether GFP⁺ neurons lacked *Isl2* (Figures 5G and 5H).

Of chimeras made by aggregating *Isl2*^{-/-}:GFP⁺ morula stage embryos with wild-type *Tg(Hb9-nLacZ)* cells, we selected those that exhibited a high proportion of wild-type (nLacZ⁺) motor neurons compared to *Isl2*^{-/-} (GFP⁺) motor neurons (Figures 5F, 5H, 5J, and 5K). As controls, similar chimeras were generated with wild-type nLacZ⁺ and wild-type *Isl2*^{+/+}:GFP⁺ embryos (Figures 5E, 5G, and 5I). In these dually marked chimeras, we sought to determine whether the presence of large numbers of wild-type cells suppressed the *Isl2* mutant phenotype. In a chimeric embryo comprised of 55% wild-type ↔ 45% *Isl2* mutant cells, 11% of the Hb9⁺ motor neurons migrated ectopically (133 of 1150 neurons examined, Figure 5K). As expected from the first set of chimeras, none were wild-type (nLacZ⁺) motor neurons (Figures 5F, 5J, and 5K). In embryos in which all thoracic motor

neurons lacked *Isl2*, ~24% of neurons were found in ectopic dorsomedial positions of the spinal cord (Table 1). Thus, if wild-type cells fail to suppress the behavior of *Isl2* mutant neurons, we would expect that in a 45% *Isl2* mutant chimera, ~11% ($0.24 \times 45\%$) of the motor neurons would be positioned ectopically. The number of ectopic motor neurons we detected, 11%, coincided precisely with the value predicted by the degree of chimerism, suggesting that wild-type motor neurons are unable to act nonautonomously to suppress the mutant motor neuron migratory phenotype. Thus, the analysis of these two *Isl2* mutant \leftrightarrow wild-type chimeric combinations provides strong evidence that *Isl2* functions in a cell-autonomous manner to permit the differentiation of visceral motor neurons.

Reducing Both *Isl2* and *Isl1* Expression Further Impairs PGC Neuronal Differentiation

In *Isl2* mutant embryos, the number of PGC neurons detected at thoracic levels was reduced but not abolished (Figures 4B and 4D; Table 1). We have found that *Isl2*, like *Isl1* (Thaler et al., 2000), can promote ectopic motor neuron differentiation when coexpressed with *Lhx3* (data not shown), suggesting these two related LIM homeodomain proteins have similar functions. This finding raised the possibility that the residual generation of PGC neurons in *Isl2* mutants might reflect the persistence of *Isl1* expression. However, since motor neuron specification is severely disrupted in constitutive *Isl1* mutants (Pfaff et al., 1996), an analysis of motor neuron subtype identity in mice carrying null mutations in both *Isl* genes is not possible.

We therefore considered an alternative means of reducing the level of *Isl1* expression in postmitotic motor neurons. Although normal numbers of spinal motor neurons are generated in *Hb9* mutant embryos, *Isl1* expression decays rapidly in postmitotic motor neurons (Arber et al., 1999; Thaler et al., 1999). This led us to analyze *Isl* protein expression, motor neuron differentiation, and subtype diversification in *Hb9*^{-/-};*Isl2*^{-/-} compound mutant embryos in which expression of both *Isl* proteins is largely absent from motor neurons. Consistent with this, in *Hb9;Isl2* double mutant embryos examined at E12.5, many neurons were detected in a ventrolateral position characteristic of spinal motor neurons, and these neurons lacked *Isl* protein (Figures 6A–6D). Analysis of PGC neuronal specification in *Hb9;Isl2* compound mutant embryos revealed a complete absence of nNOS⁺ PGC neurons (Figures 6E–6H). These findings provide evidence for a genetic interaction between *Hb9* and *Isl2* and reveal a correlation between *Isl* protein expression and activity and the progression of PGC neuronal differentiation.

Nevertheless, we were concerned that in, *Hb9;Isl2* double mutants, the further impairment of PGC neuronal differentiation could reflect the loss of *Hb9* activity. To test more directly whether *Isl1* function is required at postmitotic stages of motor neuron development, we took advantage of the finding that *Isl1* deficient motor neurons were rescued from cell death by transplanting E9.5 *Isl1* mutant mouse spinal cord into embryonic chick spinal cord. The differentiation of motor neurons and V2 interneurons in these interspecies grafts was assayed,

since in *Hb9;Isl2* double mutants we detected a dramatic upregulation of the V2 interneuron marker *Chx10* when compared with *Hb9* single mutants (Figures 6I–6L) (Arber et al., 1999; Thaler et al., 1999). The segregation of V2 interneuron and motor neuron markers proceeded normally when wild-type spinal cord tissue was grafted into chick (Figures 7A–7D). In contrast, in grafts of spinal cord tissue from *Isl1* mutants we detected a marked reduction in the number of neurons that expressed *Hb9* and a complementary increase in the number of *Chx10*⁺ V2 interneurons (Figures 7E–7I), a phenotype resembling that of *Hb9;Isl2* double mutants. Thus, a similar erosion of motor neuron identity is observed in *Hb9;Isl2* double mutants and rescued *Isl1* mutant spinal cord tissue, supporting the idea that the loss of *Isl1* expression is indeed an important contributor to the *Hb9* mutant phenotype. Together, these results suggest that a high level of *Isl* activity in newly generated motor neurons, achieved by postmitotic expression of both *Isl* proteins, is necessary for effective PGC neuronal specification.

The idea that emerges from our data, that high levels of *Isl* activity in motor neurons is permissive for PGC neuronal differentiation, predicts that ectopic expression of *Isl2* will not interfere with the assignment of visceral and somatic motor neuron fates. Consistent with this view, we found that overexpression of *Isl1* or *Isl2* did not alter the profile of somatic and PGC neuronal generation (see Supplemental Figure S2 at <http://www.neuron.org/cgi/content/full/41/3/337/DC1>, data not shown).

Later Defects in Motor Neuron Differentiation in *Hb9;Isl2* Mutant Embryos

Finally, we examined whether ventral neurons retained aspects of motor neuron character under conditions in which *Isl* protein expression was lost. To assess this issue, we first examined a hallmark of motor neuron character—the extension of axons from the spinal cord. Orthograde axonal tracing was performed by intraspinal Dil injections in *Hb9* and *Isl2* single and *Hb9;Isl2* double mutant embryos (Figures 6M–6P). Motor axons extended into the periphery in each of these mutant backgrounds (Arber et al., 1999; Thaler et al., 1999), confirming that these neurons retain this fundamental aspect of motor neuron character. In addition, expression of VACHT was retained in ventrolateral neurons in *Hb9;Isl2* double mutants (Figures 6Q–6T). The cholinergic neurotransmitter status of these neurons is indicative of motor neurons rather than V2 interneurons. Thus, two core features of spinal motor neuron differentiation, axonal extension into the periphery and cholinergic transmitter status, are retained in *Hb9;Isl2* double mutants despite the loss of *Isl* protein expression.

Pronounced defects in motor axon guidance were, however, detected in *Hb9;Isl2* mutant embryos. In wild-type embryos, thoracic nerves obeyed strict segmental boundaries (Figure 6M), but in *Isl2* and *Hb9* mutant embryos, inappropriate axonal bridges were frequently observed between segmentally arrayed motor nerves (Figures 6N and 6O). And in *Hb9;Isl2* double mutants, the incidence of this axonal misprojection defect was markedly enhanced (Figure 6P). Thus, the combined depletion of *Hb9* and *Isl2* function results in a postmitotic loss

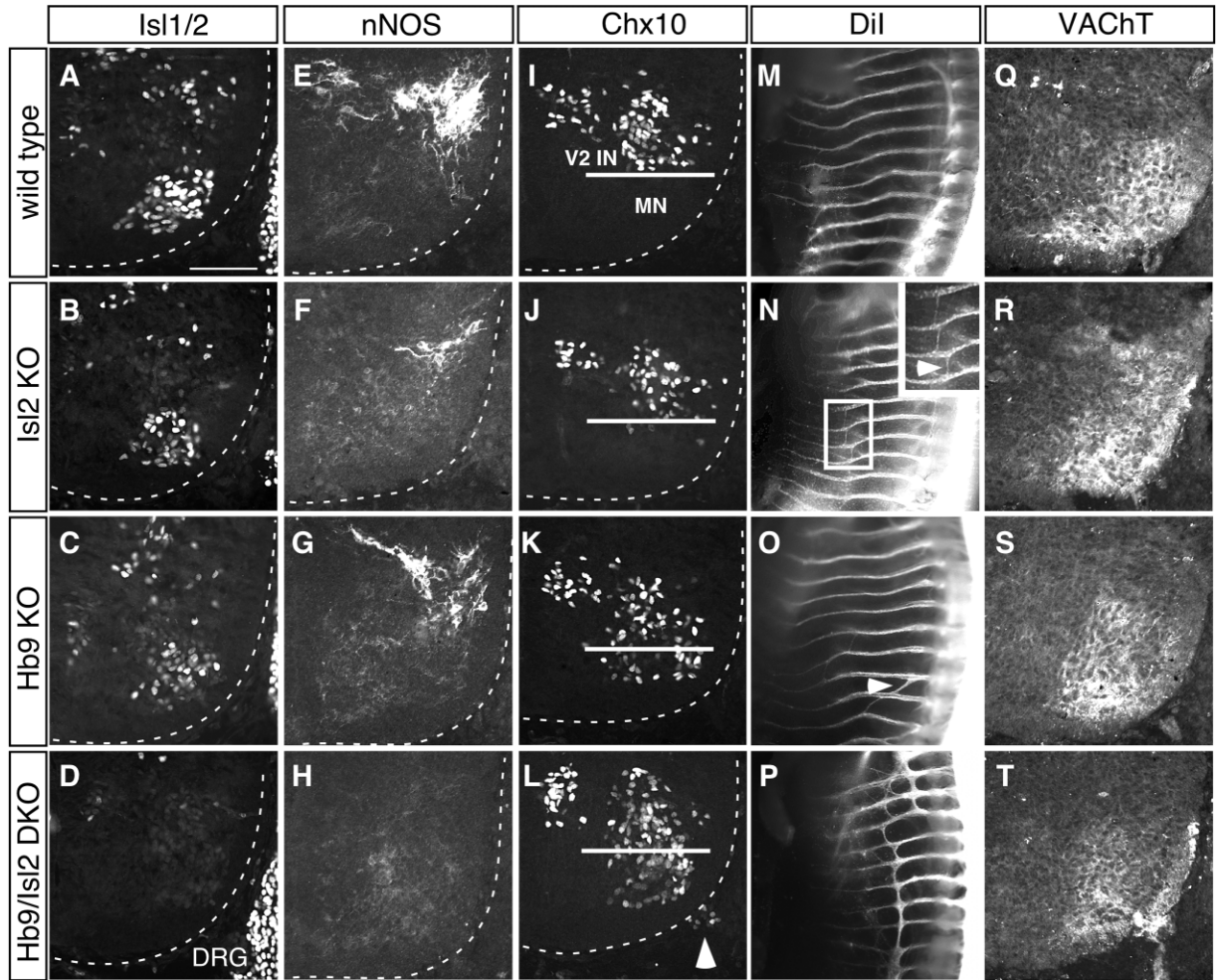


Figure 6. *Hb9;Isl2* Double Mutant Embryos Lack Visceral Motor Neurons and Display Axon Pathfinding Defects

(A–D) Pan-Isl staining (Isl1 plus Isl2) in E12.5 embryos at thoracic spinal cord levels shows a nearly complete loss of Isl1 in the ventral spinal cord of *Hb9;Isl2* double mutant embryos, while the DRG retains Isl1.
(E–H) Visceral motor neurons are labeled by nNOS in wild-type embryos (Wetts and Vaughn, 1994). The number of visceral motor neurons is reduced in both *Hb9* and *Isl2* mutants. *Hb9;Isl2* double mutant embryos fail to generate visceral motor neurons altogether.
(I–L) Chx10 labeling shows an upregulation of this V2 interneuron marker in motor neurons of *Hb9* knockouts. Chx10 expression is further increased in the motor neuron domain of *Hb9;Isl2* double mutant embryos.
(M–P) Orthograde Dil fills label all thoracic nerves.
(M) In wild-type embryos, no branches are observed in the intercostal spaces.
(N) A few slender thoracic bridges are visible in the *Isl2* knockout at fairly distal locations along the nerve (arrowhead in magnified inset).
(O) *Hb9* knockout embryos have more prominent bridges than *Isl2* mutants in the thoracic cavity (arrowhead).
(P) *Hb9;Isl2* double mutant embryos have a marked defasciculation and axon error phenotype with bridges between all levels and stunting of the brachial plexus (data not shown).
(Q–T) VACHT staining detects cholinergic cells in wild-type, *Hb9* mutant, *Isl2* mutant, and *Hb9;Isl2* double mutant embryos. Scale bar, 80 μ m (A–T).

of Isl protein expression and severely compromises the fidelity of motor axon projections into the periphery, yet retains other basic aspects of motor neuron character.

Discussion

The differentiation of motor neurons into somatic and visceral subclasses is a critical early step in the emergence of voluntary and autonomic motor functions. At thoracic levels of the spinal cord, somatic and visceral (PGC) motor neurons arise from a common progenitor population (Briscoe et al., 2000; Ericson et al., 1997; Levi-Montalcini, 1950), raising the issue of how the dis-

tinct identities of these two motor neuron subtypes are achieved. We provide evidence here that the specification of PGC motor neuron fate is dependent on a brief phase of Isl2 activity in newly generated motor neurons. In contrast, somatic motor neuron specification tolerates the lower level of Isl protein activity that persists after the loss of Isl2 function. Our data support a model in which Isl2 expression in postmitotic motor neurons confers a high level of net Isl activity that serves a permissive role in the acquisition of PGC neuronal subtype fate. We discuss these findings in the context of the role of Isl protein activity in the assignment of motor neuron subtype identity and the emerging logic by which ho-

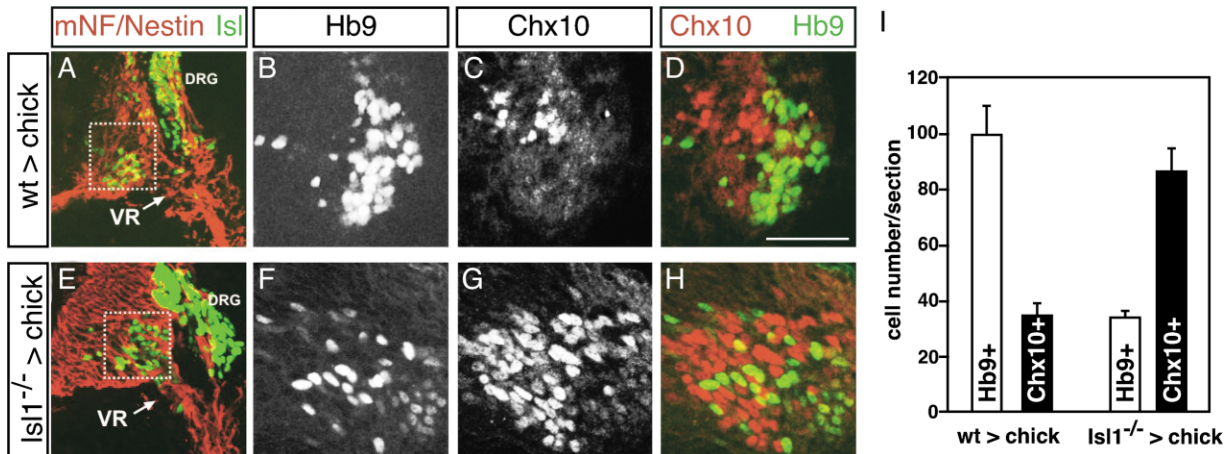


Figure 7. Analysis of Mouse>Chick Grafts Reveals a Role for Isl1 in Suppressing V2 Interneuron Genes

(A–H) Images of transverse sections through chimeric mouse>chick spinal cords: (A–D) Wild-type mouse neural tube grafted into chick spinal cord, (E–H) *Isl1* mutant mouse neural tube grafted into chick spinal cord.

(A and E) Chimeric spinal cords incubated with Isl antibody and mouse-specific anti-neurofilament (mNF) (A) or anti-nestin antisera (E). The box highlights the area of images in (B)–(D) and (E)–(H). VR, ventral root; DRG, dorsal root ganglion.

(B and F) Detection of Hb9⁺ motor neurons.

(C and G) Chx10⁺ is upregulated in *Isl1* mutants.

(D and H) Double-label overlay of images from sections in (B) and (C), and (F) and (G).

(I) Quantification (mean \pm SD) of Hb9⁺ and Chx10⁺ cells within sections of mouse tissue from wild-type mouse>chick chimeras and *Isl1* mutant mouse>chick chimeras. Scale bar, 80 μ m (B–D and F–H), 160 μ m (A–E).

meodomain protein pairs contribute to the specification of neuronal identity and diversity in the developing CNS.

A Requirement for *Isl2* in the Specification of Visceral Motor Neuron Identity

Although newly generated spinal motor neurons initially express both *Isl1* and *Isl2*, PGC neurons rapidly extinguish *Isl2* over the period of their dorsal migration, whereas most somatic motor neurons retain *Isl2* expression. Nevertheless, our analysis of motor neuron differentiation in *Isl2* mutant mice indicates that the brief phase of *Isl2* expression that occurs within postmitotic spinal motor neurons is required for efficient progression to a PGC neuronal character. The erosion of PGC neuronal identity observed in *Isl2* mutants is not associated with an overall change in the number of motor neurons but is accompanied by the emergence of more somatic-like motor neuron characteristics. The progression to somatic identity is not complete, however, since some PGC neuronal traits are retained. These findings, together with the cell-autonomous function of *Isl2* revealed from our chimera experiments, argue strongly that the loss of *Isl2* activity elicits a direct switch in the motor neuron subtype character of PGC neurons.

Although the most pronounced defects in motor neuron differentiation in *Isl2* mutants involve the loss of PGC neuronal character, our findings are suggestive of more subtle defects in somatic motor neuron differentiation at thoracic levels of the spinal cord. For example, in *Isl2* mutants, the normal segregation of somatic motor neurons into medial and lateral divisions within the MMC appears to be impaired. Since *Isl2* is the prevalent *Isl* protein in medial MMC neurons, the loss of *Isl2* function may impair their ability to segregate from *Isl1*-rich lateral MMC neurons. Alternatively, since defects in MMC seg-

regation are found preferentially at thoracic levels, where defects in PCG neuronal specification are found, the defect in MMC segregation could be an indirect consequence of the local switch from visceral to somatic neuronal fates.

The role of *Isl2* contrasts with the prominent roles for other LIM homeodomain proteins in neuronal subtype specification in the spinal cord and other regions of the vertebrate CNS (Shirasaki and Pfaff, 2002). The broad expression of *Isl2* in newly generated spinal motor neurons is not consistent with a direct instructive role in specification of motor neuron subtype identity. Rather, *Isl2* appears to serve as a permissive factor in the specification of PGC neurons. Recent studies have indicated that the profile of Hox protein expression has a critical role in the assignment of motor neuron subtype identity, with *Hoxc9* acting as a determinant of PGC neuronal identity in chick (Dasen et al., 2003). Thus, the activity of *Hoxc9* in the context of a high level of *Isl* activity, conferred by *Isl2* expression, appears to be required for effective PGC neuronal specification in the spinal cord.

Isl Activity and the Transcriptional Circuitry of Motor Neuron Diversification

The switch from PGC to somatic motor neuron character detected in *Isl2* mutant embryos is similar to that reported in *Hb9* mutant embryos, a perturbation in which *Isl1* protein levels decline rapidly in postmitotic motor neurons, leaving *Isl2* as the predominant *Isl* protein expressed (Arber et al., 1999; Thaler et al., 1999). In both *Hb9* and *Isl2* singly mutant backgrounds, PGC neuronal differentiation is impaired but not entirely blocked. These findings, combined with the high degree of sequence similarity between *Isl1* and *Isl2*, suggest that the conjoint activities of *Isl1* and *Isl2* might contribute to the

acquisition of PGC neuronal character. Consistent with this view, PGC neuronal differentiation is abolished in *Hb9;Isl2* double mutants, a condition in which both Isl1 and Isl2 protein expression is virtually extinguished from postmitotic motor neurons. Our mouse>chick spinal cord grafting data add strength to this view in that they show that the loss of Isl1 function results in an erosion of motor neuron character similar to that observed in *Hb9* mutants. Thus, a prominent function of Hb9 in postmitotic motor neurons is likely to be the maintenance of high-level Isl1 protein expression. In addition, the finding that Hb9 expression is maintained at high levels in motor neurons in *Isl2* mutant embryos indicates that Hb9 activity is not sufficient to maintain proper PGC neuronal character.

The Isl-deficient phase of postmitotic motor neuron development observed in *Hb9;Isl2* double mutants is associated with the appearance of neurons exhibiting hybrid motor neuron and V2 interneuron characteristics. Importantly, the inappropriate activation of V2-interneuron genes such as *Chx10* is more prominent in *Hb9;Isl2* mutants than in *Hb9* single mutants. Thus, under conditions of low Isl1 expression, a role for Isl2 in the suppression of V2 interneuron properties appears to be unmasked. The LIM homeodomain protein Lhx3 functions in a context-dependent manner to regulate both motor neuron and V2 interneuron differentiation (Thaler et al., 2002). Isl1 has been shown to suppress the V2 interneuron characteristics regulated by Lhx3 through direct protein-protein interactions, and a similar role for Isl2 seems likely (Thaler et al., 2002). Suppression of the interneuron-promoting function of Lhx3 could therefore underlie the need for high levels of Isl2 expression in the medial MMC, where Lhx3 is abundantly expressed. In addition, the detection of axon pathfinding errors in body wall innervating-motor neurons (MMCI) in *Isl2* mutants, and the enhancement of this phenotype when Isl1 expression is diminished, suggests that Isl activity also regulates the fidelity of somatic motor neuron axon pathfinding (Figure 8A).

Our genetic findings on *Isl2* function in motor neuron differentiation have parallels with studies in zebrafish embryos in which Isl2 expression has been blocked using antisense methodology (Segawa et al., 2001). In *Isl2*-depleted zebrafish embryos, defects in the development of both motor and sensory axons have been observed. In addition, expression of the interneuron neurotransmitter GABA was detected in primary motor neurons after overexpression of dominant-negative LIM constructs. Although these phenotypes differ in detail from those observed in *Isl2* mutant mice, some general functions of Isl2 appear to be preserved between the two organisms. For example, in both mice and fish, Isl2 seems to play a role in motor axon pathfinding. Similarly, Isl2 appears to have a conserved role in the suppression of interneuron genes.

Transcription Factor Gene Duplication and Neuronal Diversification

Our genetic evidence suggesting that Isl1 and Isl2 have additive activities in the context of motor neuron diversification in mouse is consistent with data in chick showing that Isl1 and Isl2 have similar activities in the specifi-

cation of motor neuron subtype identity in LMC neurons (Kania and Jessell, 2003). Yet, the motor neuron phenotypes of *Isl1* and *Isl2* mutant mice differ significantly (Figure 8B). These phenotypic differences in Isl protein function are likely to reflect, in part, the distinction in spatial and temporal control of the two Isl proteins. Isl1 expression precedes that of Isl2 in motor neuron differentiation, and thus the early loss of Isl1 function cannot be compensated by Isl2 activity. In this view, many of the distinct roles of Isl1 and Isl2 are likely to reflect the different profiles of expression of the two genes, although we have not ruled out that there are intrinsic differences in the activity of these two proteins.

A similar instance of transcription factor duplication is evident at other steps in spinal motor neuron development. The additive functions of *Nkx6.1* and *6.2* in progenitor cells contribute to generic motor neuron specification (Vallstedt et al., 2001), and *Lhx3* and *Lhx4* have overlapping functions in determining the distinction between motor neurons with dorsal and ventral exit points (Sharma et al., 1998). Moreover, the divergent functions of the Isl proteins in spinal motor neuron generation share features with the function of *Phox2* proteins in hindbrain motor neuron differentiation. In the developing hindbrain, differences in the timing of expression of *Phox2a* and *Phox2b* have been suggested to underlie the distinct roles of these two homeodomain proteins in the development of cranial motor neuron subpopulations (Pattyn et al., 1997, 2000).

Strategies for Visceral Motor Neuron

Specification at Different Levels of the Neural Axis

Our findings help to clarify the distinct mechanisms that specify visceral and somatic motor neuron fates at spinal and hindbrain levels of the neuraxis (Figure 8B). At hindbrain levels, separate progenitor populations give rise to somatic and visceral motor neurons (Ericson et al., 1997), whereas in the spinal cord, visceral and somatic motor neurons are generated from the same progenitor cell population (Briscoe et al., 1999, 2000; Levi-Montalcini, 1950). Thus, the differentiation of visceral and somatic motor neurons is more tightly linked at spinal cord levels with these neurons acquiring their distinguishing characteristics at a later developmental stage than their hindbrain counterparts. The distinction in developmental mechanisms of visceral motor neuron generation in the hindbrain and thoracic spinal cord could correlate with the functional subdivision of the autonomic nervous system into parasympathetic and sympathetic components located within the hindbrain and thoracic spinal cord, respectively.

The restriction of Isl protein to postmitotic motor neurons and the phenotype of the *Isl2* mutant provide further evidence that the acquisition of motor neuron subtype identity is not consolidated until well after cell cycle exit (Jessell, 2000; Shirasaki and Pfaff, 2002). Our data indicate that the early postmitotic phase of coincident Isl1 and Isl2 expression defines a critical period during which motor neuron subtype fate is still plastic. A high level of Isl protein activity, conferred by Isl2 expression, appears to permit nascent motor neurons to progress to a PGC neuronal fate. In this view, the default status of motor neurons under conditions of reduced Isl protein activity is somatic-like in character.

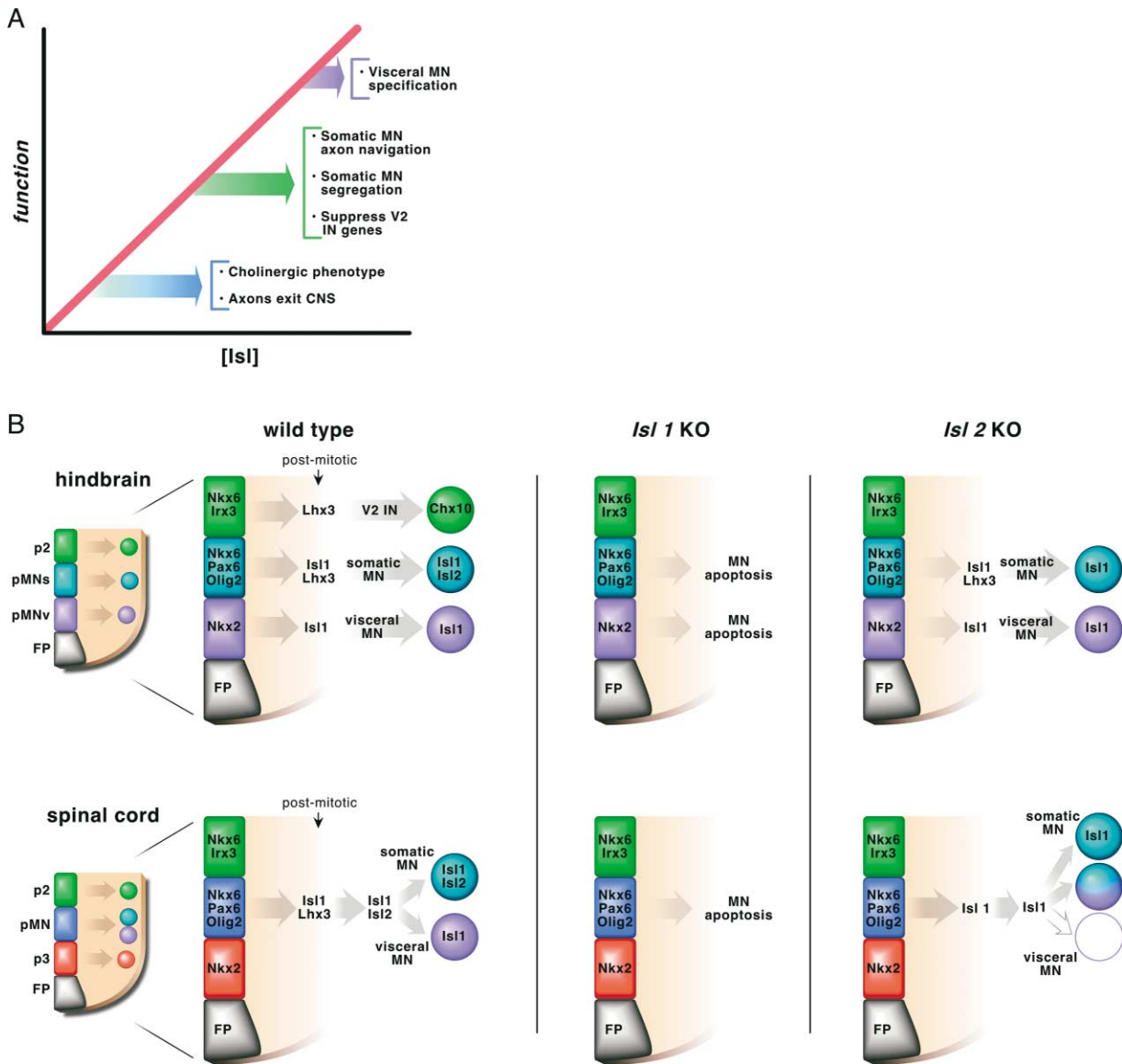


Figure 8. Summary of Isl Protein Functions during Motor Neuron Development

(A) Schematic diagram showing how increasing levels of net Isl protein activity could progressively regulate discrete aspects of spinal motor neuron differentiation. Highest levels of Isl activity, conferred by *Isl2* expression, are required for effective progression to visceral motor neuron fate, whereas the generation of somatic motor neurons tolerates the lower levels of Isl activity that persist in *Isl2* mutants.

(B) Summary of the distinct pathways of hindbrain and spinal cord visceral motor neuron specification. Discrete progenitor cell domains (rectangles) within the ventricular zone of the hindbrain and spinal cord express unique combinations of transcription factors (see Briscoe et al., 2000; Jessell, 2000; Lee and Pfaff, 2001). A permissive rather than instructive role for Isl protein activity in visceral subtype specification in the spinal cord is unmasked by our genetic studies. High Isl protein levels appear to be required in newly generated motor neurons to make the cells competent to respond to additional instructive factors that direct visceral subtype differentiation. These findings support a model in which visceral motor neurons acquire their identity during a postmitotic phase. This contrasts with the mechanisms that regulate visceral motor neuron identity in the hindbrain, where neural progenitor cells are assigned visceral and somatic motor neuron subtype fates.

Experimental Procedures

Immunocytochemistry

Embryos were isolated from pregnant females at E9.5–E15.5 and fixed in 4% paraformaldehyde in phosphate buffered saline, mounted in O.C.T (Tissue-Tek, Sakura), and cryosectioned for immunocytochemistry as described previously (Thaler et al., 1999). To generate an *Isl2*-specific antibody, a peptide corresponding to amino acids 164–181 of rat *Isl2* was synthesized and used to immunize guinea pigs. In addition, the following antibodies were used: rabbit anti-

Lhx3 (Sharma et al., 1998), rabbit anti-*Isl1/2* (Ericson et al., 1992), rabbit anti-*Isl1* (Pfaff et al., 1996), rabbit anti-Chx10 (Thaler et al., 1999), guinea pig anti-Chx10 (Thaler et al., 1999), rabbit anti-Hb9 (Thaler et al., 1999), guinea pig anti-Hb9 (Thaler et al., 1999), goat anti-VACht (Chemicon) (Weihe et al., 1996), rabbit anti-nNOS (Diasorin), and rabbit anti-LacZ (Cappel). Species-specific secondary antibodies were conjugated to FITC or Cy3 and used as recommended (Jackson Labs). Apoptotic cell death was monitored using the ApopTag Red in situ apoptosis detection kit (Intergen) and recommended protocols on cryosectioned mouse embryo tissue.

Images were obtained with a Zeiss Axioplan II microscope and a Princeton Instrument MicroMax cooled CCD camera and electronically assigned to red or green channels.

Neuronal Fills

Backlabeling of specific motor neuron subtypes was performed with 3000 MW rhodamine-dextran (Molecular Probes). Embryos were cultured in oxygenated mouse Ringers solution for 6–10 hr at room temperature to permit retrograde transport of the label then fixed for immunocytochemistry. Orthograde labeling with Dil in ethanol was performed by injection into E13.5 embryos as described previously (Sharma et al., 1998). Following Dil injection, embryos were incubated in 4% paraformaldehyde for 1 week at 37°C to permit diffusion. Dil-labeled embryos were photographed using a Zeiss SV11 dissecting microscope equipped for epifluorescence.

Mice

Isl2^{TLZ}

A 10 kb HindIII fragment of mouse genomic *Isl2* was isolated from a 129SVJ lambda library (Stratagene). From this larger clone, a 4.5 kb XhoI-BglII clone was used for gene targeting by inserting a PacI oligonucleotide into an SphI site located in the 3' UTR. A cassette with IRES-tauLacZ-NEO (Mombaerts et al., 1996) was inserted into the PacI site, electroporated into W95 mouse embryonic stem cells, and homologous recombinants were selected for generating chimeric animals using standard techniques. The genotype of these animals was monitored using the following PCR primers: 5'-GCA TCG AGC TGG GTA ATA AGC G and 5'-GAC ACC AGA CCA ACT GGT AAT GG to detect a 825 nucleotide product for LacZ; and 5'-ACA AGG GCC GGA GAT TTT TCA GAG and 5'-CTC CAG GGA CTA ACT GGG AC to detect a 650 nucleotide product for wild-type animals.

Isl2 Mutant

A neomycin resistance cassette was cloned into the KpnI-SphI sites of the 4.5 kb *Isl2* genomic clone (above), replacing the exons encoding the homeodomain and C-terminal end of *Isl2*. Homologous recombination was used to derive *Isl2*-deficient mice, as above. The genotype of animals was monitored using the following PCR primers: 5'-ACA AGG GCC GGA GAT TTT TCA GAG and 5'-GCT ACC GGT GGA TGT GGA ATG TGT to detect a 200 nucleotide mutant allele of *Isl2*; and 5'-ACA AGG GCC GGA GAT TTT TCA GAG and 5'-CTC CAG GGA CTA ACT GGG AC to detect a 650 nucleotide product for wild-type *Isl2*.

Isl1 Mutant

The generation of this line has been described previously (Pfaff et al., 1996). The genotype of animals was monitored using the following PCR primers: 5'-CGG CGC GGT CCC AGG TC and 5'-CTT CGC CCA ATA GCA GCC AGT CC to detect a 374 nucleotide mutant *Isl1* allele; and 5'-CCA AGT GCA GCA TAG GCT TCA G and 5'-ACA CAG CGG AAA CAT TCG ATG TG to detect the 84 nucleotide wild-type *Isl1*.

Hb9 Mutant

The generation of this line has been described previously (Harrison et al., 1999). The genotype of animals was monitored using the following PCR primers: 5'-GCC CCA AAG CGT CTT TGG ATC and 5'-TGG GAC ACT GAG CCC TAG TTT to detect the 1kb mutant allele; and 5'-GCT TAG CTC CCG CGA TCG CTA GGA CCC and 5'-AAG GTA CAG GAG CGG GTG GGG GCA GGT to detect the 270 nucleotide wild-type allele.

Tg(Hb9-nLacZ)

These animals contain an *Hb9* promoter and *nLacZ* reporter inserted into the 3' UTR of the *Isl2* locus using homologous recombination, as described previously (Sharma et al., 2000). The genotype of these animals was monitored using the following PCR primers: 5'-GCA TCG AGC TGG GTA ATA AGC G and 5'-GAC ACC AGA CCA ACT GGT AAT GG to detect the 825 nucleotide LacZ product; and 5'-ACA AGG GCC GGA GAT TTT TCA GAG and 5'-CTC CAG GGA CTA ACT GGG AC to detect a 650 nucleotide product indicating an *Isl2* allele lacking the reporter construct.

Tg(βactin-GFP)

The generation of these animals has been described previously (Ikawa et al., 1998). To detect the *GFP* gene, we used PCR with 5'-

AGA AAC CAT GGA CTT GTA CAG CTC GT and 5'-GGT CGC CAC CAT GGT GAG CAA primers to detect a 700 nucleotide product.

Chimeras and Mouse > Chick Grafts

To generate *Isl2^{+/-}* embryos, superovulated female *Isl2^{+/-}* or *Isl2^{-/-}*:Tg(βactin-GFP) mice were intercrossed with males of the same genotype. To generate wild-type embryos with LacZ⁺ motor neurons, wild-type females were superovulated and crossed to homozygous *Tg(Hb9-nLacZ)* males. Morula-stage embryos were flushed from the oviduct and treated with acid to remove the zona pellucida. *Isl2* mutants were aggregated to wild-type LacZ⁺ embryos by coculturing the embryos overnight. Aggregated blastocyst-stage embryos were transferred into the uterus of E2.5 pseudopregnant females, and chimeras were then recovered at E13.5 for analysis. Mouse E9.5 wild-type or *Isl1* mutant lumbar level spinal cord was dissected away from the surrounding mesoderm, grafted into the prospective brachial region of HH stage 10 chick spinal cord, and incubated for 2 days.

Acknowledgments

We are grateful to Monica Mendelsohn for expert help in generating the *Isl2* mutant mice; to Masahiro Ikawa for providing *Tg(βactin-GFP)* mice; and to Joan Vaughan and Jean Rivier for assistance in generating antibodies. We thank I. Gibbins, E. Laufer, J. Thomas, and members of the Pfaff laboratory for helpful discussions and comments on the manuscript. J.P.T. was supported by the Christopher Reeve Paralysis Foundation; S.J.K. by UCSD Medical Scientist Training Program NIHGM5 5 T32 GM07198; and S.L.P. by the J. Alexander, PEW, and Chun Foundations. T.M.J. was supported by grants from NINDS and Project ALS, and is an HHMI Investigator. This research was supported by NINDS grant RO1NS37116.

Received: July 15, 2003

Revised: November 4, 2003

Accepted: December 29, 2003

Published: February 4, 2004

References

- Arber, S., Han, B., Mendelsohn, M., Smith, M., Jessell, T.M., and Sockanathan, S. (1999). Requirement for the homeobox gene *Hb9* in the consolidation of motor neuron identity. *Neuron* 23, 659–674.
- Barber, R.P., Wetts, R., and Vaughn, J.E. (1998). Autonomic motor neuron migration and expression of nicotinamide adenine dinucleotide phosphate reduced diaphorase are dependent upon peripheral target. *J. Comp. Neurol.* 398, 568–574.
- Briscoe, J., and Ericson, J. (2001). Specification of neuronal fates in the ventral neural tube. *Curr. Opin. Neurobiol.* 11, 43–49.
- Briscoe, J., Sussel, L., Serup, P., Hartigan-O'Connor, D., Jessell, T.M., Rubenstein, J.L., and Ericson, J. (1999). Homeobox gene *Nkx2.2* and specification of neuronal identity by graded sonic hedgehog signalling. *Nature* 398, 622–627.
- Briscoe, J., Pierani, A., Jessell, T.M., and Ericson, J. (2000). A homeodomain protein code specifies progenitor cell identity and neuronal fate in the ventral neural tube. *Cell* 101, 435–445.
- Brunet, J.F., and Ghysen, A. (1999). Deconstructing cell determination: proneural genes and neuronal identity. *Bioessays* 21, 313–318.
- Callahan, C.A., Yoshikawa, S., and Thomas, J.B. (1998). Tracing axons. *Curr. Opin. Neurobiol.* 8, 582–586.
- Dasen, J.S., Liu, J.P., and Jessell, T.M. (2003). Motor neuron columnar fate imposed by sequential phases of Hox-c activity. *Nature* 425, 926–933.
- Desai, A.R., and McConnell, S.K. (2000). Progressive restriction in fate potential by neural progenitors during cerebral cortical development. *Development* 127, 2863–2872.
- Echelard, Y., Vassileva, G., and McMahon, A.P. (1994). Cis-acting regulatory sequences governing Wnt-1 expression in the developing mouse CNS. *Development* 120, 2213–2224.
- Ericson, J., Rashbass, P., Schedl, A., Brenner-Morton, S., Kawakami, A., van Heyningen, V., Jessell, T.M., and Briscoe, J. (1997).

- Pax6 controls progenitor cell identity and neuronal fate in response to graded Shh signaling. *Cell* 90, 169–180.
- Ericson, J., Thor, S., Edlund, T., Jessell, T.M., and Yamada, T. (1992). Early stages of motor neuron differentiation revealed by expression of homeobox gene *Islet-1*. *Science* 256, 1555–1560.
- Harrison, K.A., Thaler, J., Pfaff, S.L., Gu, H., and Kehrl, J.H. (1999). Pancreas dorsal lobe agenesis and abnormal islets of Langerhans in *Hlx3*-deficient mice. *Nat. Genet.* 23, 71–75.
- Hobert, O., and Westphal, H. (2000). Functions of LIM-homeobox genes. *Trends Genet.* 16, 75–83.
- Ikawa, M., Yamada, S., Nakanishi, T., and Okabe, M. (1998). 'Green mice' and their potential usage in biological research. *FEBS Lett.* 430, 83–87.
- Jessell, T.M. (2000). Neuronal specification in the spinal cord: inductive signals and transcriptional codes. *Nat. Rev. Genet.* 1, 20–29.
- Kania, A., and Jessell, T.M. (2003). Topographic motor projections in the limb imposed by LIM homeodomain protein regulation of ephrin-A:EphA interactions. *Neuron* 38, 581–596.
- Koo, S.J., and Pfaff, S.L. (2002). Fine-tuning motor neuron properties: signaling from the periphery. *Neuron* 35, 823–826.
- Lee, S.K., and Pfaff, S.L. (2001). Transcriptional networks regulating neuronal identity in the developing spinal cord. *Nat. Neurosci. Suppl.* 4, 1183–1191.
- Levi-Montalcini, R. (1950). The origin and development of the visceral system in the spinal cord of the chick embryo. *J. Morphol.* 86, 253–284.
- Lichtman, J.W., Purves, D., and Yip, J.W. (1980). Innervation of sympathetic neurones in the guinea-pig thoracic chain. *J. Physiol.* 298, 285–299.
- Livesey, F.J., and Cepko, C.L. (2001). Vertebrate neural cell-fate determination: lessons from the retina. *Nat. Rev. Neurosci.* 2, 109–118.
- Lumsden, A., and Krumlauf, R. (1996). Patterning the vertebrate neuraxis. *Science* 274, 1109–1115.
- Markham, J.A., and Vaughn, J.E. (1991). Migration patterns of sympathetic preganglionic neurons in embryonic rat spinal cord. *J. Neurobiol.* 22, 811–822.
- Mombaerts, P., Wang, F., Dulac, C., Chao, S.K., Nemes, A., Mendelsohn, M., Edmondson, J., and Axel, R. (1996). Visualizing an olfactory sensory map. *Cell* 87, 675–686.
- Pattyn, A., Morin, X., Cremer, H., Goridis, C., and Brunet, J.F. (1997). Expression and interactions of the two closely related homeobox genes *Phox2a* and *Phox2b* during neurogenesis. *Development* 124, 4065–4075.
- Pattyn, A., Hirsch, M., Goridis, C., and Brunet, J.F. (2000). Control of hindbrain motor neuron differentiation by the homeobox gene *Phox2b*. *Development* 127, 1349–1358.
- Pfaff, S., and Kintner, C. (1998). Neuronal diversification: development of motor neuron subtypes. *Curr. Opin. Neurobiol.* 8, 27–36.
- Pfaff, S.L., Mendelsohn, M., Stewart, C.L., Edlund, T., and Jessell, T.M. (1996). Requirement for LIM homeobox gene *Isl1* in motor neuron generation reveals a motor neuron-dependent step in interneuron differentiation. *Cell* 84, 309–320.
- Phelps, P.E., Barber, R.P., and Vaughn, J.E. (1988). Generation patterns of four groups of cholinergic neurons in rat cervical spinal cord: a combined tritiated thymidine autoradiographic and choline acetyltransferase immunocytochemical study. *J. Comp. Neurol.* 273, 459–472.
- Segawa, H., Miyashita, T., Hirate, Y., Higashijima, S., Chino, N., Uyemura, K., Kikuchi, Y., and Okamoto, H. (2001). Functional repression of *Islet-2* by disruption of complex with *Ldb* impairs peripheral axonal outgrowth in embryonic zebrafish. *Neuron* 30, 423–436.
- Sharma, K., Sheng, H.Z., Lettieri, K., Li, H., Karavanov, A., Potter, S., Westphal, H., and Pfaff, S.L. (1998). LIM homeodomain factors *Lhx3* and *Lhx4* assign subtype identities for motor neurons. *Cell* 95, 817–828.
- Sharma, K., Leonard, A.E., Lettieri, K., and Pfaff, S.L. (2000). Genetic and epigenetic mechanisms contribute to motor neuron pathfinding. *Nature* 406, 515–519.
- Shirasaki, R., and Pfaff, S.L. (2002). Transcriptional codes and the control of neuronal identity. *Annu. Rev. Neurosci.* 25, 251–281.
- Sockanathan, S., and Jessell, T.M. (1998). Motor neuron-derived signaling specifies the subtype identity of spinal motor neurons. *Cell* 94, 503–514.
- Thaler, J., Harrison, K., Sharma, K., Lettieri, K., Kehrl, J., and Pfaff, S.L. (1999). Active suppression of interneuron programs within developing motor neurons revealed by analysis of homeodomain factor *HB9*. *Neuron* 23, 675–687.
- Thaler, J.P., Lee, S.K., Jurata, L.W., Gill, G.N., and Pfaff, S.L. (2002). LIM factor *Lhx3* contributes to the specification of motor neuron and interneuron identity through cell-type-specific protein-protein interactions. *Cell* 110, 237–249.
- True, J.R., and Carroll, S.B. (2002). Gene co-option in physiological and morphological evolution. *Annu. Rev. Cell Dev. Biol.* 18, 53–80.
- Tsuchida, T., Ensini, M., Morton, S.B., Baldassare, M., Edlund, T., Jessell, T.M., and Pfaff, S.L. (1994). Topographic organization of embryonic motor neurons defined by expression of LIM homeobox genes. *Cell* 79, 957–970.
- Vallstedt, A., Muhr, J., Pattyn, A., Pierani, A., Mendelsohn, M., Sander, M., Jessell, T.M., and Ericson, J. (2001). Different levels of repressor activity assign redundant and specific roles to *Nkx6* genes in motor neuron and interneuron specification. *Neuron* 31, 743–755.
- Varela-Echavarría, A., Pfaff, S.L., and Guthrie, S. (1996). Differential expression of LIM homeobox genes among motor neuron subpopulations in the developing chick brain stem. *Mol. Cell. Neurosci.* 8, 242–257.
- Weihe, E., Tao-Cheng, J.H., Schafer, M.K., Erickson, J.D., and Eiden, L.E. (1996). Visualization of the vesicular acetylcholine transporter in cholinergic nerve terminals and its targeting to a specific population of small synaptic vesicles. *Proc. Natl. Acad. Sci. U.S.A.* 93, 3547–3552.
- Wetts, R., and Vaughn, J.E. (1994). Choline acetyltransferase and NADPH diaphorase are co-expressed in rat spinal cord neurons. *Neuroscience* 63, 1117–1124.
- William, C.M., Tanabe, Y., and Jessell, T.M. (2003). Regulation of motor neuron subtype identity by repressor activity of *Mnx* class homeodomain proteins. *Development* 130, 1523–1536.